Virus Spread in Networks

Piet Van Mieghem, Jasmina Omic and Rob Kooij

***Abstract*— The influence of the network characteristics on the virus spread is analyzed in a new – the N-intertwined Markov chain – model, whose only approximation lies in the application of mean field theory. The mean field approximation is quantified in detail. The N-intertwined model has been compared with the exact 2^N-state Markov model and with previously proposed "homogeneous" or "local" models. The sharp epidemic threshold τ_c, which is a consequence of mean field theory, is rigorously shown to be equal to $\tau_c = \frac{1}{\lambda_{\max}(A)}$, where $\lambda_{\max}(A)$ is the largest eigenvalue – the spectral radius – of the adjacency matrix A. A continued fraction expansion of the steady-state infection probability at node j is presented as well as several upperbounds.**

***Index Terms*— Virus spread, epidemic threshold, mean field theory, spectral radius, Markov theory**

I. Introduction

We focus on a simple continuous-time model for the spreading of a virus in a network, that was earlier considered by Ganesh *et al.* [9] and by Wang *et al.* [15] in discrete-time. The model belongs to the class of susceptible-infected-susceptible (SIS) models, that, together with the susceptible-infected-removed (SIR) models are the standard models for computer virus infections. Each node in the network is either infected or healthy. An infected node can infect its neighbors with an infection rate β, but it is cured with curing rate δ. However, once cured and healthy, the node is again prone to the virus. Both infection and curing processes are independent. Refinements like the existence of an incubation period, an infection rate that depends on the number of neighbors, a curing process that takes a certain amount of time, and other sophistications are not considered here, but we refer to e.g. [6], [2], [10], [16]. The theory of the spreads of epidemics through a network can be applied to the spread of E-mail worms and other computer viruses, the propagation of faults or failures, and, more generally, the spread of information (e.g. news, rumors, brand awareness, marketing of new products, etc.) and epidemic dissemination or/and routing in ad hoc and peer-to-peer networks.

Many authors (see e.g. [3], [11], [12], [6]) mention the existence of an epidemic threshold τ_c. If the effective spreading rate $\tau = \frac{\beta}{\delta} > \tau_c$, the virus persists and a non-zero fraction of the nodes are infected, whereas for $\tau \leq \tau_c$, the epidemic dies out. However, when the same model is exactly described via Markov theory as shown in Section III, the observation that this Markov chain (with a finite number of states) possesses an absorbing state, contradicts the existence of any threshold. For, in an irreducible Markov chain – all states are reachable from each other – the existence of an absorbing state implies that all other states are transient states and that the steady-state is the absorbing state. Moreover, the probability that the process is in a transient state, exponentially tends to zero with time. However, the convergence time T to the steady-state can be very large as shown in Section III. Ganesh *et al.* [9] give estimates of T. When the number of states grows unboundedly, major complications arise. An infinite state Markov process is considerably more complex than a finite state Markov chain as illustrated by e.g. a branching process [14, Chapter 12] where the probability of extinction is a characteristic feature that is not presented in a finite-state Markov chain. Although there is an absorbing state, in an infinite-state Markov process, there is a non-zero chance that the process never dies out. Since the exact Markov chain (see Section III) consists of 2^N– states in a network of N nodes, features of the infinite-state Markov process rapidly pop up. The apparent steady-state connected with the observation of an epidemic threshold is often termed the "metastable state" since, on a sufficiently long time-scale for finite-state systems, it disappears.

Our major motivation is to understand the influence of graph characteristics on epidemic spreading. Earlier, Wang *et al.* [15] have presented an approximate analysis from which they concluded that the threshold of the effective infection rate τ_c equals $\frac{1}{\lambda_{\max}(A)}$, where $\lambda_{\max}(A)$ is the largest eigenvalue of the adjacency matrix A of the network. This result relates – for the first time by the best of our knowledge – the epidemiological spreading to a specific characteristic, the spectral radius $\lambda_{\max}(A)$, of the network. When using mean field theory (or related averaging techniques), we rigorously show in Section IV that, in the steady-state, there is, indeed, a well-defined threshold $\tau_c = \frac{1}{\lambda_{\max}(A)}$. This result relativizes the belief of the physics society (see e.g. [1], [12]) that scale-free networks like the Internet possess a vanishingly small epidemic threshold and, hence, are vulnerable to viruses. This announcement has provoked a rush of investigations on immunization strategies for scale-free, complex networks, which is somehow questionable. In fact, since $\lambda_{\max}(A)$ is never smaller than the mean degree of the network, the class of connected Erdös-Rényi random graphs [14] possesses a far larger spectral radius than any scale-free graph with a same number of nodes N. Most complex networks are not small-world networks such that their average degree scales with the number of nodes N, which means, that for sufficiently large N, all these complex networks, not only scale-free graphs, seem prone to potential infections.

After a review of basic models for epidemics in Section II, we study the matrix structure of the infinitesimal generator Q of the exact 2^N-state Markov chain in Section III and give rather precise fitting results for the convergence time T in two limiting graphs: the complete graph and the line

Delft University of Technology, Faculty of Electrical Engineering, Mathematics and Computer Science, P.O Box 5031, 2600 GA Delft, The Netherlands. Email: {P.VanMieghem, J.S.Omic,R.E.Kooij}@ewi.tudelft.nl. Dr. ir. Kooij is also with TNO Information Communication Technology, P.O Box 5050, 2600 GB Delft.

graph. The major part is devoted to our new N-intertwined Markov model: Section IV derives the model, assesses the influence of the mean field approximation, derives precise relations and upper bounds for the steady-state. Section V and VI characterize the exponential dying out for $\tau < \tau_c$ and the role of the spectrum of A, respectively. The accuracy of the Kephart and White model is evaluated in Section VII, while Section VIII compares our model with exact computations. Section IX concludes the paper.

II. Review of some basic models

In this section, we review basic models that may help to understand the finer details of our N-intertwined model. All models are rephrased in our notation used in [14]. Other, more general models for virus spread in networks based on Markov theory are found in [10], [2].

A. The Kephart and White model

Kephart and White [11] considered a connected, regular graph[1] on N nodes where each node has degree k. The number of infected nodes in the population at time t is denoted by $I(t)$. If the population N is sufficiently large, we can convert $I(t)$ to $y(t) \equiv I(t)/N$, a continuous quantity representing the fraction of infected nodes. Hence, the implicit assumption is that the number of states is sufficiently large such that the asymptotic regime for an infinite number of states is reached. The rate at which the fraction of infected nodes changes, is determined by two processes: (a) infected nodes are being cured and (b) susceptible nodes are infected. For process (a), the cure rate of a fraction y of infected nodes is δy. The rate at which the fraction y grows in process (b) is proportional the fraction of susceptible nodes, i.e. $1-y$. For every susceptible node, the rate of infection is the product of the infection rate β per link, the number of infected neighbors (i.e. the degree k) of the node, which is ky. Combining all contributions yields the time evolution of $y(t)$ in the Kephart and White model, described by the differential equation

$$\frac{dy\left(t\right)}{dt} = \beta k y(1-y) - \delta y \tag{1}$$

whose solution is

$$y(t) = \frac{y_0 y_\infty}{y_0 + (y_\infty - y_0)e^{-(\beta k - \delta)t}} \tag{2}$$

where y_0 is the initial fraction of infected nodes whereas the steady-state fraction is $y_\infty = \lim_{t\to\infty} y(t)$ obeying $\frac{dy_\infty}{dt} = 0$.

The Kephart and White differential equation (1) is the basis of a large class of mean field models that, apart from some variations, possess the same type of solution, specified by a "steady-state" epidemic threshold,

$$\tau_{c,KW} = \frac{1}{k} \tag{3}$$

Since each node has (on average) the same degree, the Kephart and White model is also termed a "homogeneous" model. Many variations on and extensions of the Kephart and White model have been proposed (see e.g. [13]). The Kephart and White model has already appeared in earlier work (see e.g. [3]). The logistic model of population growth, that was first introduced by Verhulst in 1838 as mentioned by Daley and Gani [6, p. 20], is, in fact, the same as the simple Kephart and White model. Moreover, the simplest stochastic analogon [6, p. 56-63] – a pure birth process with transition rate $\lambda_{n,n+1} = \beta n\left(N-n\right)$– is mathematically identical to the shortest path problem [14, Chapter 16] in the complete graph with i.i.d. exponential link weights. This observation and relation to the complete graph shows that these earlier models do not take the confining way of actual virus transport into account. The central role of the network structure in the spread of viruses is the focal point of this paper.

[1]Kephart and White have modeled an Erdös-Rényi random graph $G_p\left(N\right)$ with average degree $p\left(N-1\right)$, which tends, for large N, to a regular graph. Hence, to first order in N, the properties of virus spread in Erdös-Rényi random graphs and regular graphs are the same.

B. The Model of Wang et al.

The major merit of the model of Wang *et al.* [15] is the incorporation of an arbitrary network characterized by the adjacency matrix A, which generalizes the homogeneous Kephart and White model, where the only network characteristic was the (average) degree. The discrete-time model of Wang *et al.* belongs to the class of mean field models. Their major and intriguing result is that the epidemic threshold is specified by

$$\tau_{c,\text{WCWF}} = \frac{1}{\lambda_{\max}\left(A\right)}$$

Unfortunately, this result is proved in an approximate manner which questions to what extent this remarkable result holds in general. In the sequel, we show that the Wang *et al.* model is only accurate when the effective spreading rate τ is below the "steady-state" epidemic threshold τ_c.

III. The exact 2^N-state Markov chain

We consider the virus spread in an undirected graph $G(N,L)$ characterized by a symmetric adjacency matrix A. We assume that the arrival of an infection on a link and the curing process of an infected node are independent Poisson processes with rate β and with rate δ, respectively. As soon as a node i receives an infection at time t, it is considered to be infected and infectious and in state $X_i(t) = 1$. Similarly, an infected node i is cured with rate δ, and in the healthy state $X_i(t) = 0$ at time t. At each time t a node is in one of these two states.

The state $Y\left(t\right)$ of the network at time t is defined by all possible combinations of states in which the N nodes can be at time t,

$$Y(t) = \left[\begin{array}{cccc} Y_0(t) & Y_1(t) & \ldots & Y_{2^N-1}(t) \end{array}\right]^T$$

and

$$Y_i(t) = \left\{\begin{array}{ll} 1, & i = \sum_{k=1}^{N} X_k\left(t\right) 2^{k-1} \\ 0, & i \neq \sum_{k=1}^{N} X_k\left(t\right) 2^{k-1} \end{array}\right.$$

Hence, the state space of the Markov chain is organized with $x_k \in \{0,1\}$ as

State number i	$x_N x_{N-1} ... x_2 x_1$
0	00...000
1	00...001
2	00...010
3	00..011
...	...
$2^N - 1$	11...11

The number of the states with j infected nodes is $\binom{N}{j}$. Figure 1 shows an example of the Markov state diagram in a graph with $N = 4$ nodes.

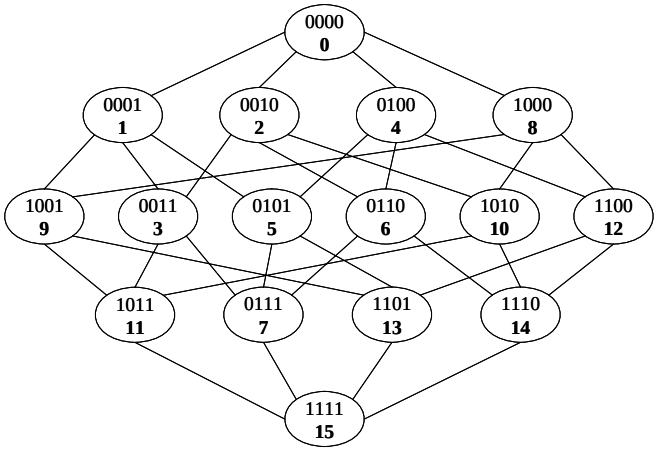

Fig. 1. The state diagram in a graph with $N = 4$ nodes and the binary numbering of the states.

The defined virus infection process is a continuous-time Markov chain with 2^N states specified by the infinitesimal generator Q with elements

$$q_{ij} = \begin{cases} \delta & \text{if } i = j + 2^{m-1}; m = 1, 2...N; x_m = 1 \\ \beta \sum_{k=1}^{N} a_{mk} x_k & \text{if } i = j - 2^{m-1}; m = 1, 2...N; x_m = 0 \\ -\sum_{k=1;k\neq j}^{N} q_{kj} & \text{if } i = j \\ 0 & \text{otherwise} \end{cases} \tag{4}$$

and $i = \sum_{k=1}^{N} x_k 2^{k-1}$. The time dependence of the probability state vector $s(t)$, with components

$$\begin{aligned} s_i(t) &= \Pr[Y(t) = i] \\ &= \Pr[X_1(t) = x_1, X_2(t) = x_2, ..., X_n(t) = x_n] \end{aligned}$$

and normalization $\sum_{i=0}^{2^N-1} s_i(t) = 1$, obeys [14, p. 182] the differential equation

$$\frac{ds^T(t)}{dt} = s^T(t)Q$$

whose solution is

$$s^T(t) = s^T(0)e^{Qt}$$

The definition of $s_i(t)$ as a joint probability distribution shows that, if we sum over all the states of all nodes except for the node j, we obtain the probability that a node j is either healthy $x_j = 0$ or infected $x_j = 1$,

$$\Pr[X_j(t) = x_j] = \sum_{i=0; i\neq j}^{2^N-1} s_i(t)$$

where, in the index $i = \sum_{k=1}^{N} x_k 2^{k-1}$, every x_k with $k \neq j$ takes both values from the set $\{0, 1\}$, while for $k = j$, $x_k = x_j$ is either 0 (healthy) or 1 (infected). Defining $v_j(t) = \Pr[X_j(t) = 1]$, then the relation between the vectors $s(t)$ and $v(t)$ is

$$v^T(t) = s^T(t)M$$

where the $2^N \times N$ matrix M contains the states in binary notation, but bit-reversed:

$$M = \begin{bmatrix} 0 & 0 & 0 & \cdots & 0 \\ 1 & 0 & 0 & \cdots & 0 \\ 0 & 1 & 0 & \cdots & 0 \\ 1 & 1 & 0 & \cdots & 0 \\ 0 & 0 & 1 & \cdots & 0 \\ \vdots & \vdots & \vdots & \vdots & \vdots \\ 1 & 1 & 1 & \cdots & 1 \end{bmatrix}$$

The binary representation of the network states determines the structure of the Q matrix. The upper triangular part of Q, denoted by Q_A, depends on the adjacency matrix elements a_{ij}, while the lower triangular part Q_δ does not. The diagonal elements of any Q matrix are the negative sum of the row elements, such that $Q_{\text{diag}} = \text{diag}\left(q_{00}, q_{11}, \ldots, q_{2^{N-1},2^{N-1}}\right)$ with $q_{jj} = -\sum_{k=1;k\neq j}^{N} q_{kj}$ as in (4). It is thus instructive to write Q as a sum of three matrices $Q = Q_\delta + Q_A + Q_{\text{diag}}$. The structure of the matrix Q_δ is shown in the Fig. 2, where the block matrix $B(j) = \delta I_{2^j \times 2^j}$ and the nondefined elements are zeros. This nested structure is the consequence of the binary representation.

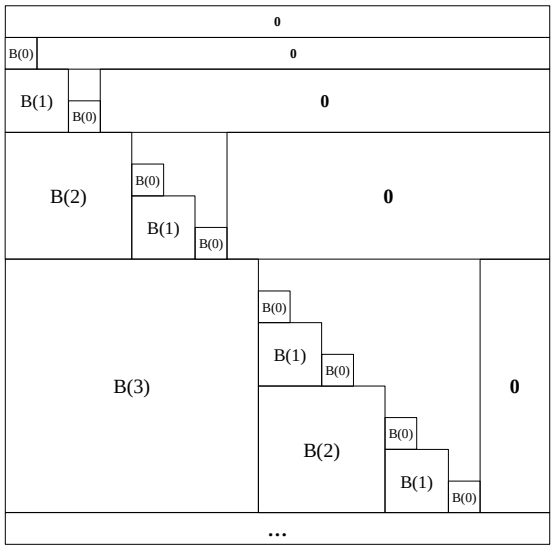

Fig. 2. The lower triangular part Q_δ of the infinitesimal generator Q.

The matrix Q_A is shown in Fig. 3. The block matrices $C(j)$ in Q_A are diagonal matrices of size $2^j \times 2^j$ with diagonal elements depending on the adjacency matrix A. The first row of the matrix Q is zero, and as a consequence the largest block is $C(N-1)$. The elements of Q_A depend on the indices i, j where $i = \sum_{k=1}^{N} x_k 2^{k-1}$ as $Q_A(i, j) = \beta \sum_{k=1}^{N} a_{mk} x_k$ where $i = j - 2^{m-1}; m = 1, 2...N; x_m = 0$. The exact 2^N- state Markov chain has an absorbing state because the

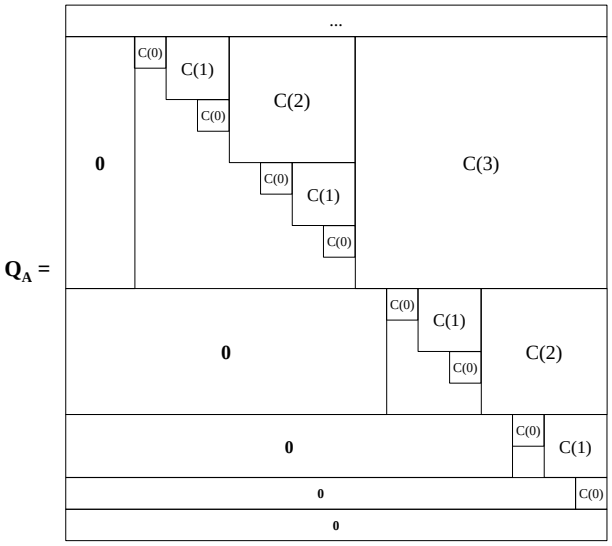

Fig. 3. The upper triangular part Q_A of Q.

first row in Q is a zero row and the absorbing state is the zero state in which all nodes are healthy. The steady-state is just this absorbing state, with steady-state vector $s_\infty = \pi = (1, 0, \ldots, 0)$. The probability state vector requires the insights in the eigenstructure of Q because [7]

$$s(t) = s(0)e^{Qt} = \pi + \sum_{k=1}^{2^N-1} e^{\lambda_k t} \sum_{m=0}^{n_k-1} r_{k,m} \frac{t^m}{m!}$$

where n_k denotes the multiplicity of the eigenvalue λ_k (with $\mathrm{Re}\,\lambda_k < 0$) and the vector $r_{k,m}$ is related to the left- and right eigenvector belonging to λ_k and the initial conditions. Since $v_j(t) = \left(s^T(t)\,M\right)_j = \sum_{k=0}^{2^N-1} s_k M_{kj}$ is a sum of certain rows of $s(t)$, we may write

$$v_j(t) = \sum_{k=1}^{2^N-1} e^{\lambda_k t} \sum_{m=0}^{n_k-1} \left(\sum_{i \in M_j} (r_{k,m})_i \right) \frac{t^m}{m!}$$

where M_j denotes the j-th column in the matrix M. Let μ_j be the largest eigenvalue λ_k of the set where $(r_{k,m})_i \neq 0$, then $v_j(t)$ is dominated (for not too small t) by

$$v_j(t) \sim e^{\mu_j t} \sum_{m=0}^{n_{\mu_j}-1} \gamma_m \frac{t^m}{m!} \qquad (5)$$

which shows that a "bell-shape" distribution of $v_j(t)$ can only occur if that largest eigenvalue $\mu_j < 0$ has a multiplicity larger than 1.

A. Spectrum of Q

For all infinitesimal generators, it holds that $\det Q = 0$, and, hence, the largest eigenvalue is $\lambda = 0$.

Theorem 1: For $\beta = 0$, the eigenvalues of the matrix Q, defined by (4), are $\lambda(Q_{\beta=0}) = -k\delta$ with multiplicity $\binom{N}{k}$, where $0 \leq k \leq N$.

Proof: For $\beta = 0$, the infinitesimal generator $Q = Q_\delta + Q_{\text{diag}} + Q_A$ reduces to the lower-triangular matrix $Q_\delta + Q_{\text{diag}}$, whose eigenvalues are identical to the diagonal elements of Q_{diag}, which are multiples of δ. In fact, the structure of Q_δ shows that each block row j has a row sum equal to $k\delta$ for $1 \leq k \leq N$ whose value appears $\binom{j}{k-1}$ times. Hence, $Q_{\beta=0}$ has an eigenvalue at $\lambda = -k\delta$ with multiplicity $\sum_{j=0}^{N-1} \binom{j}{k-1} = \binom{N}{k}$. These contain all the non-zero eigenvalues of $Q_{\beta=0}$ because $\sum_{k=1}^{N} \binom{N}{k} = 2^N - 1$. □

For small values of τ, Q tends thus to a discrete, binomial spectrum. Fig. 4 illustrates that, also for larger τ, the spectrum of Q for the complete graph K_N is still discrete[2], containing many eigenvalues with high multiplicity.

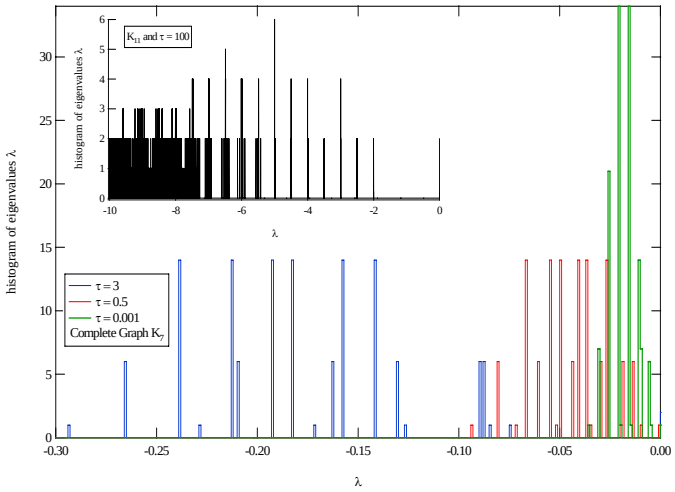

Fig. 4. (in color) The histogram eigenvalues λ of Q of the in the complete graph K_N for three values of τ gives the number of times an eigenvalue λ occurs. The insert shows the spectrum of K_{11} for an extremely high $\tau = 100$.

Proposition 2: For constant δ and increasing β (and $\tau = \frac{\beta}{\delta}$), the eigenvalues of Q shift, on average, to more negative values than those of $Q_{\beta=0}$.

Proof: We apply Gershgorin's Theorem[3] to $Q = Q_\delta + Q_{\text{diag}} + Q_A$, where $Q_A = \beta T_A$ and T_A only contains (non-zero) integer elements related to the adjacency matrix A as observed from (4). Hence, $q_{ii} < 0$ decreases with β which implies that both the center position and the possible range of each eigenvalue $\lambda_i(Q)$ increases with β. □

Corollary 3: The eigenvalues of Q for the complete graph K_N and line graph spread over the largest, respectively smallest possible range among all connected graphs. The maximum possible range of the real part of eigenvalues of Q for any connected graph is $\left(-\frac{(\beta N+\delta)^2}{2\beta}, 0\right]$

Proof: From $Q_A = \beta T_A$, defined in the proof of Theorem 2, it follows that the maximum possible sum of row elements occurs for K_N (all $a_{ij} = 1$ except for $a_{ii} = 0$) and the minimum one for line graph (only one 1-element on each row in the adjacency matrix A). Gershgorin's Theorem then provides the first statement. Since the maximum eigenvalue

[2]Random matrices of this size exhibit an almost continuous spectrum.

[3]Every eigenvalue of a matrix B lies in at least one of the circular discs with centers b_{jj} and radii $R_j = \sum_{k=1;k\neq j} |b_{jk}|$. For any infinitesimal generator Q, Gershgorin's Theorem shows that $|\lambda_i - q_{ii}| \leq |q_{ii}|$ and that the maximum possible interval for real eigenvalues of Q is $[0, 2\max_i |q_{ii}|]$.

range thus occurs for a complete graph, we consider in the Q-matrix for K_N the i-th row with k one-bits in the binary representation. The row elements, except from the diagonal element, represents the transitions from and to a state with $N-k$ healthy and k infected nodes. The row sum of these positive elements equals $\beta k(N-k)+k\delta$, and, hence, $q_{ii} = -\beta k(N-k)-k\delta$. Optimizing with respect to k proves the corollary. □

As shown in the Appendix, also for the line graph, the maximum of the diagonal elements q_{ii} can be computed.

Yet, there are open questions regarding the spectrum of Q. (a) Although Q is not symmetric, computations reveal that all eigenvalues of Q are real (and negative). (b) Perturbation theory of Q for small β (or τ) expresses the eigenvalues in terms of those of $Q_{\beta=0}$ and of the corresponding right- and left-eigenvectors of $Q_{\beta=0}$. However, the multiplicity of the eigenvalues of $Q_{\beta=0}$ further complicates the perturbation analysis. (c) The recursive block-structure (due to the binary representation) of Q needs to be exploited.

In the sequel of this section, we confine to explicit computation of the Q matrix for two extreme types of graphs, the complete graph which has the smallest average hopcount (or the fastest virus penetration), and the line graph that possesses the largest possible average hopcount.

1) The complete graph K_N: Fig. 5 shows the four largest eigenvalues of Q for the complete graph K_N for $N = 5, 8$ and 10. The second largest eigenvalue seems the only eigenvalue that increases – contrary to the expectations of Gershgorin's Theorem – roughly exponentially in τ and with rate increasing for increasing size N. This second largest eigenvalue determines the speed of convergence towards the steady-state. Fig. 5 also shows that, initially for small τ, the third and fourth eigenvalue are the same and bifurcate (see dots) into distinct values roughly around $\tau_c = \frac{1}{\lambda_{\max}(A)} = \frac{1}{N-1}$. Hence, (5) indicates that below τ_c, the dominant eigenvalue is simple causing exponential decay, while above τ_c, it has multiplicity larger than 1 creating a bell-shape. This observation agrees with the figures in Section VIII.

In Fig. 6, the eigenvalues of Q for all computable complete graphs (up to $N = 13$) have been numerically calculated. The second largest eigenvalue seems well fitted (for $\tau \geq 0.05$) by

$$\lambda_2 = -\delta\, e^{-b(\tau)L} \tag{6}$$

where $L = \binom{N}{2}$ denotes the number of links in the complete graph K_N. The dependence on τ is approximately given by $b(\tau) \approx 0.17\tau(1+2\tau)$. Assuming that the scaling law (6) of λ_2 holds for any N, the convergence time T of the virus spread in K_N towards the steady-state (the zero state), defined by $r_2 e^{-|\lambda_2|T} = 10^{-\epsilon}$ is found as $T = O\left(e^{b(\tau)L}\right) = O\left(e^{\frac{b(\tau)}{2}N^2}\right)$. In other words, for large size N and $\tau > 0$, the convergence time T is so large that convergence towards the zero state is in reality never reached, which explains the appearance of the so-called "metastable state".

Ganesh *et al.* [9] show that, for $\tau < \tau_c$ – a regime that is not covered by (6) –, the mean epidemic lifetime $E[T]$ scales as $O(\log N)$ while, for $\tau > \tau^* > \tau_c$ where τ^* is the generalized isoperimetric constant, $E[T] = O\left(e^{N^a}\right)$, for some constant a. If we may extrapolate (6) to large N, it shows that the constant $a = 2$ for K_N.

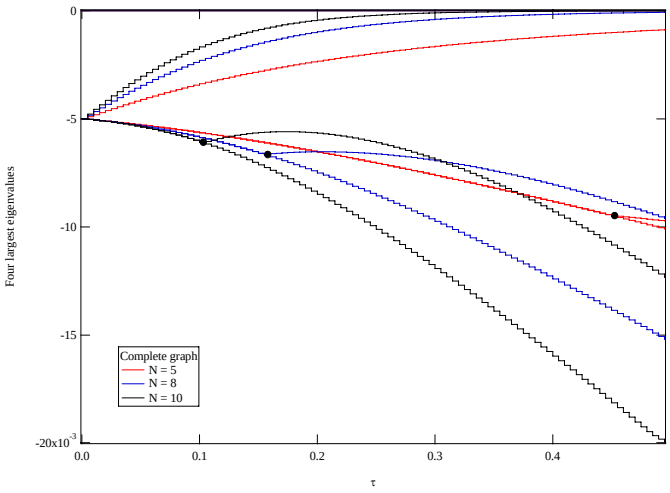

Fig. 5. The four largest eigenvalues of the infinitesimal generator Q for the complete graph with size $N = 5, 8$ and 10 as a function of τ with $\delta = 5\ 10^{-3}$. The second largest eigenvalues are increasing with τ as $\lambda_2(5) \approx -\delta e^{-3.5\tau}$,$\lambda_2(8) \approx -\delta e^{-8.8\tau}$ and $\lambda_2(10) \approx -\delta e^{-14.7\tau}$.

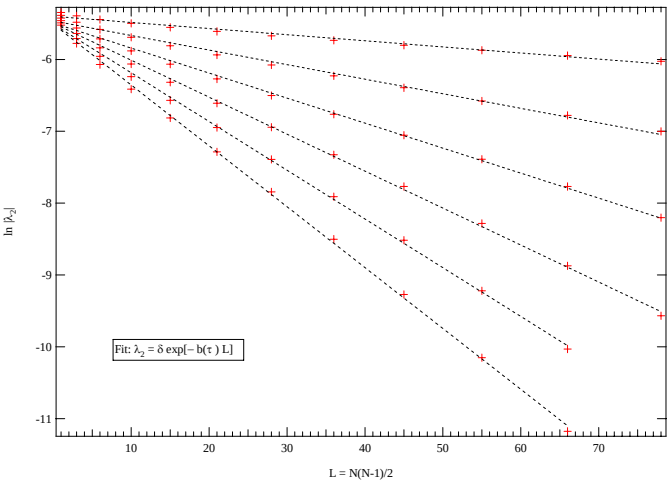

Fig. 6. The logarithm of $-\lambda_2$ versus the number links in K_N for $\tau = 0.05, 0.1, 0.15, \ldots, 0.3$ and $\delta = 5\ 10^{-3}$.

2) The line graph: Fig. 7 plots the second largest eigenvalue λ_2 of Q for the line graph. The largest eigenvalue of the adjacency matrix A of the line graph, where each row has precisely one non-zero element in the upper triangular part of A, is $\lambda_{\max}(A) = 2\cos\left(\frac{\pi}{N+1}\right) < 2$. Fig. 7 (axis on the right) also shows the epidemic threshold of the line graph $\tau_c = \frac{1}{\lambda_{\max}(A)} > \frac{1}{2}$ versus N. As observed from Fig. 7, the curves λ_2 increase very slowly with N. Via curve fitting in the range $N \in [8, 13]$, we found that $\lambda_2(\tau, N) \approx -\delta e^{-\tau(1.184+0.0413N)}$, which shows the exponential dependence on τ (accurate) and the less accurate dependence on N. If extrapolation to large N is allowed, the convergence time T of the virus spread in the line graph towards the steady-state (the zero state) is $T = O\left(\frac{1}{\lambda_2}\right) = O\left(e^{\tau(1.184+0.0413N)}\right)$, which is considerably

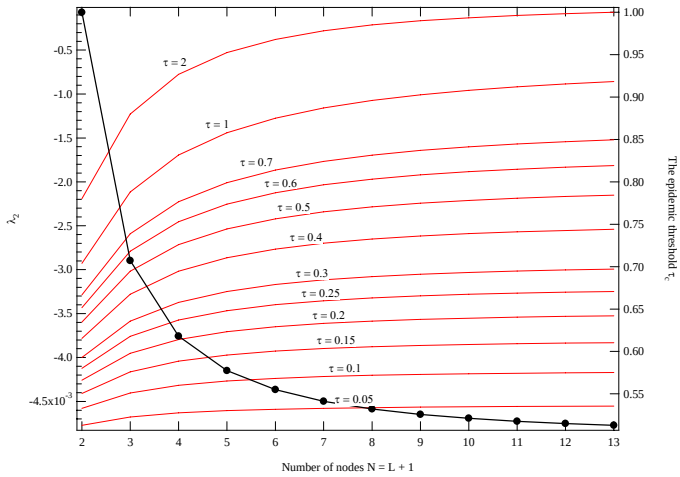

Fig. 7. The second largest eigenvalue λ_2 of Q in the line graph versus the number of nodes N for various τ and $\delta = 5\ 10^{-3}$. The epidemic threshold τ_c is shown in dotted line on the right hand side axis.

smaller than in K_N, the other extreme case.

B. Conclusion

An upper and lower bound on the spectrum of any graph are given. Via fitting, we complement the scaling laws of Ganesh *et al.* [9]. The matrix computations (on a PC) are limited to $N = 13$. Simulations and the analytic matrix computations are, within the simulation accuracy, identical. This observation allows us to replace the matrix computations by simulations beyond graph sizes of $N = 13$.

IV. N-Intertwined Continuous Markov Chains with 2 States

By separately observing each node, we will model the virus spread in a bi-directional network specified by a symmetric adjacency matrix A. Every node i at time t in the network has two states: infected with probability $\Pr[X_i(t) = 1]$ and healthy with probability $\Pr[X_i(t) = 0]$. At each moment t, a node can only be in one of two states, thus $\Pr[X_i(t) = 1] + \Pr[X_i(t) = 0] = 1$. If we apply Markov theory straight away, the infinitesimal generator $Q_i(t)$ of this two-state continuous Markov chain is,

$$Q_i(t) = \begin{bmatrix} -q_{1;i} & q_{1;i} \\ q_{2;i} & -q_{2;i} \end{bmatrix}$$

with $q_{2;i} = \delta$ and

$$q_{1;i} = \beta \sum_{j=1}^{N} a_{ij} 1_{\{X_j(t)=1\}}$$

where the indicator function $1_x = 1$ if the event x is true else it is zero. The coupling of node i to the rest of the network is described by an infection rate $q_{1;i}$ that is a random variable, which essentially makes the process doubly stochastic. This observation is crucial. For, using the definition of the infinitesimal generator [14, p. 181],

$$\Pr[X_i(t+\Delta t) = 1 | X_i(t) = 0] = q_{1;i}\Delta t + o(\Delta t)$$

the continuity and differentiability shows that this process is not Markovian anymore. The random nature of $q_{1;i}$ is removed by an additional conditioning to all possible combinations of rates, which is equivalent to conditioning to all possible combinations of the states $X_j(t) = 1$ (and their complements $X_j(t) = 0$) of the neighbors of node i. Hence, the number of basic states dramatically increases. Eventually, after conditioning each node in such a way, we end up with a 2^N- state Markov chain, defined earlier in Section III.

Instead of conditioning, we replace the actual, random infection rate by an effective or average infection rate, which is basically a mean field approximation,

$$E[q_{1;i}] = E\left[\beta \sum_{j=1}^{N} a_{ij} 1_{\{X_j(t)=1\}}\right] \tag{7}$$

In general, we may take the expectation over the rate β, the network topology via the matrix A and the states $X_j(t)$. Since we assume that both the infection rate β and the network are constant and given, we only average over the states. Using $E[1_x] = \Pr[x]$ (see e.g. [14]), we replace $q_{1;i}$ by

$$E[q_{1;i}] = \beta \sum_{j=1}^{N} a_{ij} \Pr[X_j(t) = 1]$$

which results in an effective infinitesimal generator,

$$\overline{Q_i(t)} = \begin{bmatrix} -E[q_{1;i}] & E[q_{1;i}] \\ \delta & -\delta \end{bmatrix}$$

The effective $\overline{Q_i(t)}$ allows us to proceed with Markov theory. Denoting $v_i(t) = \Pr[X_i(t) = 1]$ and recalling that $\Pr[X_i(t) = 0] = 1 - v_i(t)$, the Markov differential equation [14, (10.11) on p. 182] for state $X_i(t) = 1$ turns out to be non-linear

$$\frac{dv_i(t)}{dt} = \beta \sum_{j=1}^{N} a_{ij} v_j(t) - v_i(t) \left(\beta \sum_{j=1}^{N} a_{ij} v_j(t) + \delta\right) \tag{8}$$

Each node obeys a differential equation as (8),

$$\begin{cases} \frac{dv_1(t)}{dt} = \beta \sum_{j=1}^{N} a_{1j} v_j(t) - v_1(t) \left(\beta \sum_{j=1}^{N} a_{1j} v_j(t) + \delta\right) \\ \frac{dv_2(t)}{dt} = \beta \sum_{j=1}^{N} a_{2j} v_j(t) - v_2(t) \left(\beta \sum_{j=1}^{N} a_{2j} v_j(t) + \delta\right) \\ \vdots \\ \frac{dv_N(t)}{dt} = \beta \sum_{j=1}^{N} a_{Nj} v_j(t) - v_N(t) \left(\beta \sum_{j=1}^{N} a_{Nj} v_j(t) + \delta\right) \end{cases}$$

Written in matrix form, with $V(t) = \begin{bmatrix} v_1(t) & v_2(t) & \cdots & v_N(t) \end{bmatrix}^T$, we arrive at

$$\frac{dV(t)}{dt} = \beta A V(t) - \text{diag}(v_i(t)) (\beta A V(t) + \delta u) \tag{9}$$

where u is the all-one vector and $\text{diag}(v_i(t))$ is the diagonal matrix with elements $v_1(t), v_2(t), \ldots, v_N(t)$.

We rewrite (9) with $V(t) = \text{diag}(v_i(t))\, u$ as

$$\begin{aligned} \frac{dV(t)}{dt} &= \beta A V(t) - \delta \text{diag}(v_i(t))\, u - \text{diag}(v_i(t))\, \beta A V(t) \\ &= (\beta A - \delta I) V(t) - \beta \text{diag}(v_i(t))\, A V(t) \end{aligned}$$

or

$$\frac{dV(t)}{dt} = (\beta \text{diag}(1 - v_i(t))A - \delta I)V(t) \quad (10)$$

The time-continuous analogue of Wang *et al.* [15] would be $\frac{dV(t)}{dt} = (\beta A - \delta I)V(t)$, which thus ignores the important non-linear term $\beta \text{diag}(v_i(t))AV(t)$, and, consequently as shown in Section IV-B, it limits the validity to $\tau \leq \tau_c$.

An extension of the N-intertwined model where the curing and infection rates are node specific is

$$\frac{dV(t)}{dt} = A\text{diag}(\beta_i)V(t) - \text{diag}(v_i(t))(A\text{diag}(\beta_i)V(t) + \Delta)$$

where the curing rate vector is $\Delta = (\delta_1, \delta_2, \ldots, \delta_N)$. We note that $A\text{diag}(\beta_i)$ is, in general, not symmetric anymore, unless A and $\text{diag}(\beta_i)$ commute, in which case the eigenvalue $\lambda_i(A\text{diag}(\beta_i)) = \lambda_i(A)\beta_i$ and both β_i and $\lambda_i(A)$ have a same eigenvector x_i. In case the curing and infection rates are link specific, the adjacency matrix A can be extended to that of a multi-link graph, where $a_{ij} = a_{ji}$ is an integer counting the number of links (representing the strength of infection) between node i and node j. Generally, A can be a non-negative real, symmetric matrix where each $a_{ij} = a_{ji}$ contains the strength of the infection of link (i, j) in units of a constant β.

A. The mean field approximation

At first glance, the averaging process – replacing $q_{1;i}$ in (7) by its mean $E[q_{1;i}]$ – seems quite accurate, because a sum S_N of independent indicators (Bernoulli random variables) is close – exactly if all Bernoulli random variables have the same distribution – to a binomial random variable, whose standard deviation $\sigma_{S_N} = \sqrt{\text{Var}[S_N]} = O\left(\sqrt{N}\right)$ is small compared to the mean $E[S_N] = O(N)$. The latter implies that the random variable S_N is closely approximated by its mean[4] for large N.

However, $\frac{q_{1;i}}{\beta} = \sum_{j=\text{neighbor}(i)} 1_{\{X_j(t)=1\}} \in \{0, 1, \ldots, d_i\}$ is a sum of *dependent* indicators. In addition, if N is large, $q_{1;i}$ does not always increase with N. Indeed, $q_{1;i} \leq \beta d_{\max}(A)$ and the maximum degree $d_{\max}(A)$ in a graph can be independent of N, for example, in the line graph where $d_{\max} = 2$ for any N.

We will first elaborate on the dependence. Let us consider the time-dependent random variable $S_i(t) = 1_{\{X_i(t)=1\}}$, which is 1 if node i is infected, else it is zero. If the node i is infected ($X_i(t) = 1$) , $S_i(t)$ can change from 1 to 0 with curing rate δ. If the node i is healthy ($X_i(t) = 0$), $S_i(t)$ can change from 0 to 1 with rate $\beta \sum_{j=1}^N a_{ij} 1_{\{X_j(t)=1\}}$. The change of S_i in a sufficiently small time interval Δt is

$$\frac{S_i(t + \Delta t) - S_i(t)}{\Delta t} = (1 - S_i(t))\beta \sum_{j=1}^N a_{ij} 1_{\{X_j(t)=1\}} - \delta S_i(t)$$

After taking the expectation of both sides, we obtain (with $E[S_i(t)] = \Pr[X_i(t) = 1] = v_i(t)$)

$$\frac{v_i(t + \Delta t) - v_i(t)}{\Delta t} = \beta \sum_{j=1}^N a_{ij} v_j(t) - \delta v_i(t) - E\left[1_{\{X_i(t)=1\}} \beta \sum_{j=1}^N a_{ij} 1_{\{X_j(t)=1\}}\right]$$

Since $a_{ii} = 0$, only the case where $j \neq i$ appears in the remaining expectation, which is

$$\begin{aligned} E\left[1_{\{X_i(t)=1\}} 1_{\{X_j(t)=1\}}\right] &= E\left[1_{\{X_i(t)=1\} \cap \{X_j(t)=1\}}\right] \\ &= \Pr[X_i(t) = 1, X_j(t) = 1] \\ &= c_{ij}(t) \Pr[X_i(t) = 1] \end{aligned}$$

where the conditional probability $c_{ij}(t) = \Pr[X_j(t) = 1 | X_i(t) = 1]$. Hence, when $\Delta t \to 0$, we arrive at

$$\frac{dv_i(t)}{dt} = \beta \sum_{j=1}^N a_{ij} v_j(t) - v_i(t) \left(\beta \sum_{j=1}^N a_{ij} c_{ij}(t) + \delta\right)$$

Assuming that the graph is connected,

$$\Pr[X_j(t) = 1 | X_i(t) = 1] \geq \Pr[X_j(t) = 1]$$

because a given infection at node i cannot negatively influence the probability of infection at node j. When comparing with (8), we observe that the mean field approximation implicitly makes the assumption of independence that $\Pr[X_j(t) = 1, X_k(t) = 1] = \Pr[X_j(t) = 1] \Pr[X_k(t) = 1]$. Hence, the positive correlation is not incorporated appropriately. As a consequence, the rate of change in $\frac{dv_i(t)}{dt}$ is always overestimated. *The N-intertwined Markov chain thus upperbounds the exact probability $v_i(t)$ of infection.*

Next, we will address the effect on the size N by computing the variance of $q_{1;i}$, $\text{Var}[q_{1;i}] = E[q_{1;i}^2] - (E[q_{1;i}])^2$. First, we have

$$\begin{aligned} E[q_{1;i}^2] &= E\left[\beta \sum_{j=1}^N a_{ij} 1_{\{X_j(t)=1\}} \beta \sum_{k=1}^N a_{ik} 1_{\{X_k(t)=1\}}\right] \\ &= \beta^2 \sum_{j=1}^N \sum_{k=1}^N a_{ik} a_{ij} E\left[1_{\{X_j(t)=1\}} 1_{\{X_k(t)=1\}}\right] \\ &= \beta^2 \sum_{j=1}^N \sum_{k=1}^N a_{ik} a_{ij} \Pr[X_j(t) = 1, X_k(t) = 1] \end{aligned}$$

or, in terms of the conditional probabilities,

$$E[q_{1;i}^2] = \beta^2 \sum_{j=1}^N \sum_{k=1}^N a_{ik} a_{ij} \Pr[X_j(t) = 1 | X_k(t) = 1] \Pr[X_k(t) = 1]$$

[4]More precisely, the central limit theorem for a sum $S_N = \sum_{j=1}^N R_j$ of *independent* random variables $R_1, \ldots, R_N$, each with finite variance $\text{Var}[R_j]$ (and small compared to $\text{Var}[S_N]$) states that, for large N,

$$\Pr\left[\frac{S_N - E[S_N]}{\sqrt{\sum_{j=1}^N \text{Var}[R_j]}} \leq x\right] \to \frac{1}{\sqrt{2\pi}} \int_{-\infty}^x e^{-\frac{t^2}{2}} dt$$

Applied to *independent* indicators with $\text{Var}\left[1_{\{X_j(t)=1\}}\right] = \Pr[X_j(t) = 1](1 - \Pr[X_j(t)]) \leq E\left[1_{\{X_j(t)=1\}}\right]$ shows that, for $x \geq 0$ and large N,

$$\Pr\left[|S_N - E[S_N]| \geq x\sqrt{E[S_N]}\right] \leq \frac{1}{\sqrt{2\pi}} \int_x^\infty e^{-\frac{t^2}{2}} dt \overset{\text{large } x}{\approx} \frac{e^{-\frac{x^2}{2}}}{x\sqrt{2\pi}}$$

where the last step follows after (successive) partial integration and retaining the $O\left(x^{-1}\right)$ term in the series for large x. Hence, for *independent indicators*, large deviations from the mean are very unlikely.

Since $\Pr[X_j(t)=1|\,X_k(t)=1] \leq 1$, an upperbound of $E\left[q_{1;i}^2\right]$ is

$$E\left[q_{1;i}^2\right] \leq \beta^2 d_i \sum_{k=1}^{N} a_{ik} \Pr[X_k(t)=1] = \max[q_{1;i}]\, E[q_{1;i}] \tag{11}$$

The variance of $q_{1;i}$ is

$$\begin{aligned}\text{Var}\ [q_{1;i}] = \beta^2 \sum_{j=1}^{N} a_{ij} \Pr[X_j(t)=1]\,(1-\Pr[X_j(t)=1]) \\ + 2\beta^2 \sum_{j=1}^{N}\sum_{k=j+1}^{N} a_{ik}a_{ij}\left(c_{kj}(t)-v_j(t)\right)v_k(t)\end{aligned} \tag{12}$$

Since $c_{kj}(t) \geq v_j(t)$ as argued above, the second double sum consists of non-negative terms such that the variance Var$[q_{1;i}]$ is larger than in the case of independent random variables (where the double sum disappears). This fact is not in favor of the mean field approximation since larger variations around the mean $E[q_{1;i}]$ can occur which makes the mean a less good approximation for the random variable $q_{1;i}$. In particular, (12) shows that standard deviation $\sqrt{\text{Var}[q_{1;i}]} = O(N)$, whereas the standard deviation scales as $O\left(\sqrt{N}\right)$ in case of independence! Especially in graphs with bounded maximum degree (such as the line graph), $\sqrt{\text{Var}[q_{1;i}]}$ may not decrease sufficiently fast in N compared to $E[q_{1;i}]$. Thus, we expect deviations between the N-intertwined and the exact model in those graphs to be largest.

For small τ (and t large enough to ignore the initial conditions), $\Pr[X_k(t)=1] \leq \varepsilon$ and (12) shows that the double sum is $O\left(\varepsilon^2\right)$. Hence, for small τ, the situation is close to the independence case, in which mean field theory performs generally well. An upperbound for Var$[q_{1;i}]$ follows from (11) such that the coefficient of variation

$$\frac{\sqrt{\text{Var}\ [q_{1;i}]}}{E[q_{1;i}]} \leq \sqrt{\frac{\max[q_{1;i}]}{E[q_{1;i}]} - 1}$$

This shows, that for large τ where $E[q_{1;i}] \to \max[q_{1;i}]$, the coefficient of variation is small, again in favor of the mean field approximation. *Hence, we expect that the deviations between the N-intertwined and the exact model are largest for intermediate values of τ.* As shown in Section VIII, in some τ-region around τ_c, large deviations are indeed found.

The two observations, dependence and absence of a limiting process towards the mean as N increases, complicate a more precise assessment of the averaging process at this point. Since the mean field approximation is the only approximation made, a comparison of the non-linear model (9) with the exact 2^N-state solution in Section VIII further quantifies the effect of the mean field approximation.

Finally, the mean field approximation also excludes information about the joint probability of states,

$$\Pr[X_1(t)=n_1, X_2(t)=n_2, \ldots, X_N(t)=n_N]$$

where all $n_j \in \{0,1\}$, as in the 2^N– state Markov chain.

B. The steady-state under the mean field approximation

Assuming that the steady-state exists, we can calculate the steady-state probabilities of infection for each node. The steady-state, denoted by $v_{j\infty}$, implies that $\left.\frac{dv_j(t)}{dt}\right|_{t\to\infty} = 0$, and thus we obtain from (8) for each node j,

$$\beta \sum_{j=1}^{N} a_{ij} v_{j\infty} - v_{i\infty}\left(\beta \sum_{j=1}^{N} a_{ij} v_{j\infty} + \delta\right) = 0$$

Since all the diagonal elements of the adjacency matrix A are zero, $a_{jj}=0$, we find

$$v_{i\infty} = \frac{\beta \sum_{j=1}^{N} a_{ij} v_{j\infty}}{\beta \sum_{j=1}^{N} a_{ij} v_{j\infty} + \delta} = 1 - \frac{1}{1+\tau \sum_{j=1}^{N} a_{ij} v_{j\infty}} \tag{13}$$

This nodal steady-state is the ratio of the (average) infection rate induced by the node's direct neighbors $\sum_{j=1}^{N} a_{ij} v_{j\infty}$ over the total (average) rate of both the competing infection and curing process. Since $a_{jj}=0$, (13) is equal to the steady-state probability in a two-state, continuous Markov chain (see e.g. [14, p. 196]), which exemplifies the local (or nodal) character of our N-intertwined Markov model. We observe the trivial solution $v_{i\infty}=0$ for all i, which means that eventually, all nodes will be healthy. On the other hand, if $\delta=0$, then all $v_{i\infty}=1$, or slightly more precise, (13) shows that $v_{i\infty} = 1 - O\left(\tau^{-1}\right)$ for large τ. Of course, if there is no curing at all ($\delta=0$), all nodes will eventually be infected almost surely.

Lemma 4: In a connected graph, either $v_{i\infty}=0$ for all i nodes, or none of the components $v_{i\infty}$ is zero.

Proof: If $v_{i\infty}=0$ for one node i in a connected graph, then it follows from (13) that $\sum_{j=1}^{N} a_{ij} v_{j\infty} = 0$ which is only possible provided $v_{j\infty}=0$ for all neighbors j of node i. Applying this argument repeatedly to the neighbors of neighors in a connected graph proves the lemma. □

Apart from the exact steady-state $v_{i\infty}=0$ for all i, the non-linearity gives rise to a second solution, coined as the "metastable state". That second, non-zero solution can be interpreted as the fraction of time that a node is infected while the system is in the "metastable state", i.e. there is a long-lived epidemic.

Theorem 5: For any effective spreading rate $\tau = \frac{\beta}{\delta} \geq 0$, the non-zero steady-state infection probability of any node i in the N-intertwined model can be expressed as a continued fraction

$$v_{i\infty} = 1 - \cfrac{1}{1+\tau d_i - \tau \sum_{j=1}^{N} \cfrac{a_{ij}}{1+\tau d_j - \tau \sum_{k=1}^{N} \cfrac{a_{jk}}{1+\tau d_k - \tau \sum_{q=1}^{N} \cfrac{a_{kq}}{1+\tau d_q - \ddots}}}} \tag{14}$$

where $d_i = \sum_{j=1}^{N} a_{ij}$ is the degree of node i. Consequently, the exact steady-state infection probability of any node i is bounded by

$$0 \leq v_{i\infty} \leq 1 - \frac{1}{1+\tau d_i} \tag{15}$$

Proof: We rewrite (13) as

$$\begin{aligned} v_{i\infty} &= 1 - \frac{1}{1+\tau\sum_{j=1}^{N} a_{ij} v_{j\infty}} \\ &= 1 - \frac{1}{1+\tau d_i - \tau\sum_{j=1}^{N} a_{ij}\left(1-v_{j\infty}\right)} \\ &\leq 1 - \frac{1}{1+\tau d_i} \end{aligned}$$

since $\tau\sum_{j=1}^{N} a_{ij}\left(1-v_{j\infty}\right) \geq 0$ because $v_{j\infty} \in [0,1]$ for all j. This proves (15).

We proceed further by introducing $1 - v_{j\infty} = \frac{1}{1+\tau\sum_{k=1}^{N} a_{jk} v_{k\infty}}$, such that

$$\begin{aligned} v_{i\infty} &= 1 - \frac{1}{1+\tau d_i - \tau\sum_{j=1}^{N} \frac{a_{ij}}{1+\tau\sum_{k=1}^{N} a_{jk} v_{k\infty}}} \\ &= 1 - \frac{1}{1+\tau d_i - \tau\sum_{j=1}^{N} \frac{a_{ij}}{1+\tau d_j - \tau\sum_{k=1}^{N} a_{jk}\left(1-v_{k\infty}\right)}} \\ &\leq 1 - \frac{1}{1+\tau d_i - \tau\sum_{j=1}^{N} \frac{a_{ij}}{1+\tau d_j}} \end{aligned}$$

This bound improves on (15). The third iteration gives

$$v_{i\infty} = 1 - \frac{1}{1+\tau d_i - \tau\sum_{j=1}^{N} \frac{a_{ij}}{1+\tau d_j - \tau\sum_{k=1}^{N} \frac{a_{jk}}{1+\tau d_k - \tau\sum_{q=1}^{N} a_{kq}\left(1-v_{q\infty}\right)}}}$$

Ignoring $\sum_{q=1}^{N} a_{kq}(1-v_{q\infty}) \geq 0$ yields a new upper bound that sharpens the previous upper bound of the second iteration. Each iteration provides a tighter upper bound by putting $\sum_{q=1}^{N} a_{kq}(1-v_{q\infty}) = 0$ in the deepest fraction. Continuing the process leads to an infinite continued fraction expansion (14) for $v_{i\infty}$. □

The continued fraction stopped at iteration k includes the effect of virus spread up to the $(k-1)$-hop neighbors of node i. As illustrated in Fig. 8 (and typical for other graphs that we have simulated), a few iterations in (14) already give an accurate approximation. The accuracy seems worst around $\tau = \tau_c$.

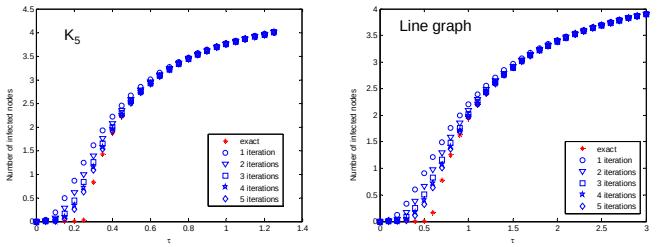

Fig. 8. Difference between the exact result and the k-iterations ($1 \leq k \leq 5$) of (14) for the complete graph and line graph (both with $N = 5$ nodes) versus the effective infection rate τ.

Additional insight can be gained from (9), which in steady-state reduces to

$$AV_\infty - \text{diag}\left(v_{i\infty}\right)\left(AV_\infty + \frac{1}{\tau}u\right) = 0$$

Define the vector $w = AV_\infty + \frac{1}{\tau}u$, then

$$w - \frac{1}{\tau}u = \text{diag}\left(v_{i\infty}\right) w$$

or

$$\left(I - \text{diag}\left(v_{i\infty}\right)\right) w = \frac{1}{\tau}u$$

Ignoring the absence of curing ($\delta = 0$ or $\tau \to \infty$), the bound (15) shows that $v_{i\infty}$ cannot be one such that the matrix $(I - \text{diag}\left(v_{i\infty}\right)) = \text{diag}(1 - v_{i\infty})$ is invertible. Hence,

$$\begin{aligned} w &= \text{diag}\left(\frac{1}{1-v_{i\infty}}\right)\frac{1}{\tau}u \\ &= \frac{1}{\tau}\left[\begin{array}{cccc} \frac{1}{1-v_{1\infty}} & \frac{1}{1-v_{2\infty}} & \cdots & \frac{1}{1-v_{N\infty}} \end{array}\right]^T \end{aligned}$$

and we end up with the equation

$$\frac{1}{\tau}\left[\begin{array}{cccc} \frac{v_{1\infty}}{1-v_{1\infty}} & \frac{v_{2\infty}}{1-v_{2\infty}} & \cdots & \frac{v_{N\infty}}{1-v_{N\infty}} \end{array}\right]^T = AV_\infty$$

Further, we expand each element as $\frac{v_{i\infty}}{1-v_{i\infty}} = \sum_{k=1}^{\infty} v_{i\infty}^k$, where the geometric series always converges since $v_{i\infty} < 1$. With the notation $V_\infty^k = \left[\begin{array}{cccc} v_{1\infty}^k & v_{2\infty}^k & \cdots & v_{N\infty}^k \end{array}\right]^T$, we arrive at the steady-state equation

$$\frac{1}{\tau}V_\infty + \frac{1}{\tau}\sum_{k=2}^{\infty} V_\infty^k = AV_\infty \tag{16}$$

Lemma 6: There exists a value $\tau_c = \frac{1}{\lambda_{\max}(A)} > 0$ and for $\tau < \tau_c$, there is only the trivial steady-state solution $V_\infty = 0$. Beside the $V_\infty = 0$ solution, there is a second, non-zero solution for all $\tau > \tau_c$. For $\tau = \tau_c + \varepsilon$ where $\varepsilon > 0$ is an arbitrary small constant, $V_\infty = \varepsilon x$ where x is the eigenvector belonging to the largest eigenvalue of the adjacency matrix A.

Proof: Theorem 5 shows that the only solution at $\tau = 0$ is the trivial solution $V_\infty = 0$. Let $V_\infty = \varepsilon x$, where $\varepsilon > 0$ is an arbitrary small constant and each component $x_i \geq 0$. Introduced in (16) gives, after division by ε,

$$Ax = \frac{1}{\tau}x + \frac{\varepsilon}{\tau}x^2 + O\left(\varepsilon^2\right)$$

For sufficiently small $\varepsilon > 0$, the steady-state equations reduce to the eigenvalue equation

$$Ax = \frac{1}{\tau}x \tag{17}$$

which shows that x is an eigenvector of A belonging to the eigenvalue $\frac{1}{\tau}$. Since A is a non-negative matrix, the Perron-Frobenius Theorem [14, p. 451] states that A has a positive largest eigenvalue $\lambda_{\max}(A)$ with a corresponding eigenvector whose elements are all positive and there is only one eigenvector of A with non-negative components. Hence, if $\frac{1}{\tau} = \lambda_{\max}(A) > 0$, then x (and any scaled vector $V_\infty = \varepsilon x$) is the eigenvector of A belonging to $\lambda_{\max}(A)$. If $\tau < \frac{1}{\lambda_{\max}(A)} = \tau_c$, then $\frac{1}{\tau}$ cannot be an eigenvalue of A and the only possible solution is $x = 0$, leading to the trivial solution $V_\infty = 0$. For $\tau > \tau_c$, Theorem 5 provides the non-zero solution of (13). □

Canright *et al.* [4] proposed the eigenvector centrality (EVC) measure of a spreading power of a node

$$e_i = \frac{1}{\lambda_{\max}}\sum_{j=\text{neighbor}(i)} e_j$$

where e_k is the spreading power of a node k. Written in our notation as $v_{i\infty} = \frac{1}{\lambda_{\max}} \sum_{j=1}^{N} a_{ij} v_{j\infty}$, the EVC is recognized as the component representation of the eigenvalue equation (17) for $\tau = \tau_c$. The steady-state infection probability is the long-run fraction of time during which the node is infected. The higher the probability $v_{i\infty}$, the faster the node i is prone to infection and the more important its role is in further spreading. This Markov steady-state interpretation may explain the term centrality analogously as the betweenness centrality of a node.

In passing by, we note that, by combining Theorem 5 and Lemma 6, a continued fraction expansion of the (scaled) largest eigenvector in any graph is found from (14) for $\tau = \tau_c = \frac{1}{\lambda_{\max}(A)}$.

Lemma 7: For any effective spreading rate $\tau = \frac{\beta}{\delta} \geq 0$, the components $v_{i\infty}$ of the steady-state infection probability vector obey

$$\sum_{i=1}^{N} \left(\frac{1}{1 - v_{i\infty}} - \tau d_i \right) v_{i\infty} = 0 \tag{18}$$

Proof: By summing all rows in (16), which is equivalent to multiplication of both sides in (16) by the all-one vector u^T yields

$$\frac{1}{\tau} \sum_{i=1}^{N} v_{i\infty} + \frac{1}{\tau} \sum_{k=2}^{\infty} \sum_{i=1}^{N} v_{i\infty}^{k} = u^T A V_\infty$$
$$= D^T V_\infty = \sum_{i=1}^{N} d_i v_{i\infty}$$

where $D = \begin{bmatrix} d_1 & d_2 & \cdots & d_N \end{bmatrix}^T$ is the degree vector. After rewriting the k-sum, we arrive at (18). □

Equation (18) is obeyed for the trivial solution $v_{i\infty} = 0$ and, if $v_{i\infty} = 1 - \frac{1}{\tau d_i}$. In the case of regular graphs (where $d_i = d$ for all $1 \leq i \leq N$), both $v_{i\infty} = 0$ and $v_{i\infty} = 1 - \frac{1}{\tau d}$ are exact solutions of (13). This shows that, in certain cases, the continued fraction (14) can be simplified.

The fraction $y_\infty(\tau) = \frac{1}{N} \sum_{i=1}^{N} v_{i\infty}(\tau)$ of infected nodes in the network, based on the estimate $v_{i\infty} \approx 1 - \frac{1}{\tau d_i}$, is

$$y_\infty(\tau) \approx 1 - \frac{1}{\tau N} \sum_{i=1}^{N} \frac{1}{d_i} \tag{19}$$

Numerical computations in Fig. 9 assess the quality of the approximation (19).

Lemma 8: For all i, $v_{i\infty} = 1 - \frac{1}{\tau d_i}$ cannot be a solution of (13) for $\tau \leq \frac{1}{d_{(2)}}$ where $d_{(2)} > d_{\min}$ is the second smallest degree in the graph G.

Proof: Indeed, $1 - v_{i\infty} = \frac{1}{\tau d_i} \leq \frac{d_{(2)}}{d_i}$ leads for $d_i = d_{\min} < d_{(2)}$ to $v_{i\infty} < 0$, which is impossible. □

The strict inequality $d_{(2)} > d_{\min}$ is important. Lemma 8 explains that larger variations in the degree lead to worse results of (19) in Fig. 9.

Lemma 9: In a connected graph G with minimum degree $d_{\min}$ and for $\tau \geq \frac{1}{d_{\min}}$, a lower bound of $v_{i\infty}$ for any node i equals

$$1 - \frac{1}{1 + \frac{d_i}{d_{\min}}(\tau d_{\min} - 1)} \leqslant v_{i\infty} \tag{20}$$

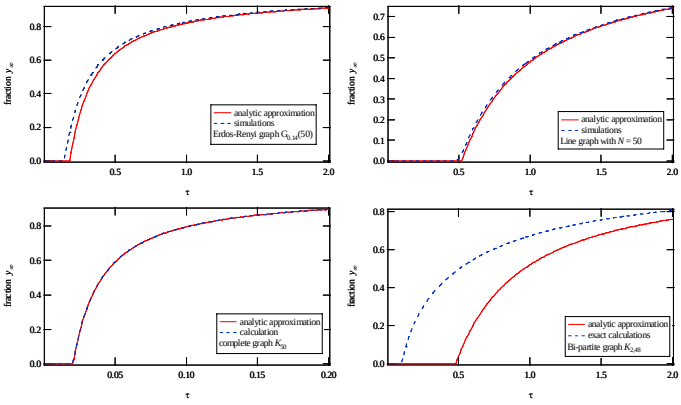

Fig. 9. Comparison of (19) and exact computations or precise simulations for different type of graphs with $N = 50$ nodes

Proof: Lemma 4 and Lemma 6 show that, for $\tau > \tau_c$, there exists a non-zero minimum $v_{\min} = \min_{1 \leq i \leq N} \{v_{i\infty}\} > 0$ of steady-state infection probabilities, which obeys (13), assuming that this minimum $v_{\min}$ occurs at node i,

$$v_{\min} = 1 - \frac{1}{1 + \tau \sum_{j=1}^{N} a_{ij} v_{j\infty}} \geq 1 - \frac{1}{1 + \tau \sum_{j=1}^{N} a_{ij} v_{\min}}$$
$$= 1 - \frac{1}{1 + \tau d_i v_{\min}} \geq 1 - \frac{1}{1 + \tau d_{\min} v_{\min}}$$

From the last inequality, it can be shown that

$$v_{\min} \geq 1 - \frac{1}{\tau d_{\min}} \tag{21}$$

which is only larger than zero provided $\tau > \frac{1}{d_{\min}} \geq \tau_c$. Introducing the bound (21), we also have for each node

$$v_i \geq v_{\min} \geq 1 - \frac{1}{1 + \tau d_i v_{\min}} \geqslant 1 - \frac{1}{1 + \frac{d_i}{d_{\min}}(\tau d_{\min} - 1)}$$

which is (20). □

For $d_{\min} = 1$ the lowest possible lower bound for node i is

$$v_{i\infty} \geqslant 1 - \frac{1}{1 + (\tau - 1) d_i}$$

Finally, by combining the upper bound (15) and the lower bound (20) for $\tau \geq \frac{1}{d_{\min}}$, we find that $v_{i\infty}$ belongs to the interval

$$1 - \frac{1}{1 + \frac{d_i}{d_{\min}}(\tau d_{\min} - 1)} \leqslant v_{i\infty} \leqslant 1 - \frac{1}{1 + \tau d_i}$$

This shows clearly that for $\tau \to \infty$ variations between all values of v_i for all i will tend to 0.

C. An example: the complete bi-partite graph $K_{m,n}$

The adjacency matrix of the complete bi-partite graph $K_{m,n}$ is, with $N = m + n$,

$$A_{K_{m,n}} = \begin{bmatrix} O_{m \times m} & J_{m \times n} \\ J_{n \times m} & O_{n \times n} \end{bmatrix} \tag{22}$$

The bi-partite graph $K_{m,n}$ may represent a set of m servers and n clients. Let us now solve the equation (10) for the bi-partite graph

$$\frac{dV(t)}{dt} = \beta \text{diag}(1 - v_i(t)) \begin{bmatrix} O_{m\times m} & J_{m\times n} \\ J_{n\times m} & O_{n\times n} \end{bmatrix} \begin{bmatrix} V_{m\times 1} \\ V_{n\times 1} \end{bmatrix} - \delta \begin{bmatrix} I_{m\times m} & O_{m\times n} \\ O_{n\times m} & I_{n\times n} \end{bmatrix} \begin{bmatrix} V_{m\times 1} \\ V_{n\times 1} \end{bmatrix}$$

After some manipulations, we find

$$\frac{1}{\beta}\frac{d}{dt}\begin{bmatrix} V_{m\times 1} \\ V_{n\times 1} \end{bmatrix} = \begin{bmatrix} -\frac{1}{\tau}V_{m\times 1} + \text{diag}(1 - v_i)_m J_{m\times n} V_{n\times 1} \\ \text{diag}(1 - v_i)_n J_{n\times m} V_{m\times 1} - \frac{1}{\tau}V_{n\times 1} \end{bmatrix}$$

With $J_{m\times n} = u_{m\times 1}u_{1\times n}$, we rewrite

$$\begin{aligned} \text{diag}(1 - v_i)_m J_{m\times n} V_{n\times 1} &= \text{diag}(1 - v_i)_m u_{m\times 1}u_{1\times n}V_{n\times 1} \\ &= (u_{m\times 1} - V_{m\times 1})\, u_{1\times n}V_{n\times 1} \end{aligned}$$

With $Ny_n = u_{1\times n}V_{n\times 1}$, the first m rows

$$\begin{aligned} \frac{1}{\beta}\frac{d}{dt}V_{m\times 1} &= -\frac{1}{\tau}V_{m\times 1} + (u_{m\times 1} - V_{m\times 1})\, Ny_n \\ &= -\left(\frac{1}{\tau} + Ny_n\right) V_{m\times 1} + Ny_n u_{m\times 1} \end{aligned}$$

reduce to m identical equations, from which it is tempting to conclude that $v_i = w_m$ for all $1 \le i \le m$ and for all t. However, this assumption is only valid if all initial conditions $v_i(0)$ are the same. Only in that case,

$$\frac{1}{\beta}\frac{dw_m}{dt} = -\left(\frac{1}{\tau} + Ny_n\right) w_m + Ny_n$$

Similarly for the n last equations, we have with $v_i = w_n$ for all $m + 1 \le i \le N$, that

$$\frac{1}{\beta}\frac{dw_n}{dt} = -\left(\frac{1}{\tau} + Ny_m\right) w_n + Ny_m$$

With $Ny_n = u_{1\times n}V_{n\times 1} = nw_n$ and $Ny_m = u_{1\times m}V_{m\times 1} = mw_m$, we arrive at

$$\begin{cases} \frac{1}{\beta}\frac{dw_m}{dt} = -\left(\frac{1}{\tau} + nw_n\right) w_m + nw_n \\ \frac{1}{\beta}\frac{dw_n}{dt} = -\left(\frac{1}{\tau} + mw_m\right) w_n + mw_m \end{cases} \tag{23}$$

The steady-state obeys

$$\begin{cases} 0 = -\left(\frac{1}{\tau} + nw_{n\infty}\right) w_{m\infty} + nw_{n\infty} \\ 0 = -\left(\frac{1}{\tau} + mw_{m\infty}\right) w_{n\infty} + mw_{m\infty} \end{cases}$$

These equations hold in general for $K_{m,n}$ because the steady-state does not dependent on the initial conditions. Substituting $w_{m\infty} = \frac{nw_{n\infty}}{\left(\frac{1}{\tau} + nw_{n\infty}\right)}$ from the first equation into the second, yields

$$w_{n\infty} = \frac{mn - \frac{1}{\tau^2}}{\left(\frac{1}{\tau} + m\right) n} \tag{24}$$

and, introduced in the first equation,

$$w_{m\infty} = \frac{mn - \frac{1}{\tau^2}}{\left(\frac{1}{\tau} + n\right) m} \tag{25}$$

Hence, all components of the steady-state $V_\infty = \begin{bmatrix} w_{m\infty}u_{m\times 1} \\ w_{n\infty}u_{n\times 1} \end{bmatrix}$ are found.

V. The time evolution of epidemics

Suppose that all $v_i(t)$ are sufficiently small to ignore the term $\text{diag}(v_i(t))\,\beta AV(t)$ in (10), the time-dependent solution is

$$V(t) = e^{(\beta A - \delta I)t}V(0)$$

Since an adjacency matrix has the eigenvalue decomposition $A = U\Lambda U^T$, where $\Lambda = \text{diag}(\lambda_j)$ and $\{\lambda_j\}_{1\le j\le N}$ is the set of eigenvalues of A, and where the orthonormal matrix U has the eigenvectors of A as columnvectors (see e.g. [14, Appendix A]), we obtain

$$B = \beta A - \delta I = U(\beta\Lambda - \delta I)U^T$$

or $B = U\text{diag}(\beta\lambda_j - \delta)U^T$. Thus,

$$V(t) = U\text{diag}\left(e^{(\beta\lambda_j - \delta)t}\right)U^T V(0)$$

and, in order for $V(t)$ to be a probability vector, we must require that all eigenvalues $\beta\lambda_j - \delta \le 0$ or that $\lambda_j \le \frac{1}{\tau}$ for all j. This again leads to the requirement that $\tau \le \frac{1}{\lambda_{\max}(A)}$. The analysis shows that, in the regime $\tau \le \frac{1}{\lambda_{\max}(A)}$, the probability vector $V(t)$ tends exponentially fast to zero.

Ganesh *et al.* [9, Theorem 3.1] and Durrett [8] have bounded the probability that the virus spread process is not (yet) in the absorbing state as

$$\Pr[X(t) \ne 0] \le \sqrt{N\|X(0)\|_1}\, e^{(\beta\lambda_{\max}(A) - \delta)t}$$

where the norm (see e.g. [14, Section A.3]) $\|X(0)\|_1 = \sum_{j=1}^N X_j(0)$. Since $\Pr[X(t) \ne 0]$ is related to $V(t)$ and the largest component of $V(t)$ precisely decays proportionally to $e^{(\beta\lambda_{\max}(A) - \delta)t}$, we may expect that the non-linear N-intertwined model is fairly accurate for $\tau \le \tau_c = \frac{1}{\lambda_{\max}(A)}$, as also confirmed by simulations presented in Section VIII.

VI. The fraction $y(t)$ of infected nodes and the role of the spectrum of A

The sum $y(t) = \frac{1}{N}\sum_{i=1}^N v_i(t)$ gives the fraction of infected nodes in the network. Summing (8) over all i is equivalent to right multiplication of $V(t)$ by u^T because $\sum_{i=1}^N v_i(t) = u^T V(t)$. Then, we find from (10) that

$$\begin{aligned} \frac{du^T V(t)}{dt} &= u^T(\text{diag}(1 - v_i(t))\,\beta A - \delta I)\,V(t) \\ &= \beta(u - V(t))^T AV(t) - \delta u^T V(t) \end{aligned}$$

Since $u^T A = D^T$ because $A = A^T$, we can write

$$\frac{d}{dt}\left(u^T V(t)\right) = (\beta D - \delta u)^T V - \beta V^T AV \tag{26}$$

Invoking the eigenvalue decomposition $A = U\Lambda U^T$ of the symmetric adjacency matrix leads to

$$\begin{aligned} \frac{d}{dt}\left(u^T V(t)\right) &= (\beta D - \delta u)^T V - \beta\left(U^T V\right)^T \Lambda\left(U^T V\right) \\ &= (\beta D - \delta u)^T V - \beta\sum_{j=1}^N \lambda_j(A)\, z_j^2 \end{aligned} \tag{27}$$

where z_j is the j-th component of the vector $U^T V$: the scalar product $V.x_j$ or the projection of the vector V onto

the j-th eigenvector x_j of A. We have that $0 \leq V^T AV = \sum_{j=1}^{N} \lambda_j(A) z_j^2$.

Equation (27) shows that the zero eigenvalues in the adjacency matrix of a graph do not contribute to the infected fraction $y(t) = \frac{u^T V}{N}$ of nodes. In general, a matrix has a zero eigenvalue if its determinant is zero. A determinant is zero if two rows are identical or if some of the rows are linearly dependent. For example, two rows are identical if two distinct nodes are connected to a same set of nodes. Since the elements a_{ij} of an adjacency matrix A are only 0 or 1, linear dependence of rows here occurs every time the sum of a set of rows equals another row in the adjacency matrix. For example, consider the sum of two rows. If n_1 is connected to the set S_1 of nodes and n_2 is connected to the distinct set S_2, where $S_1 \cap S_2 = \varnothing$ and $n_1 \neq n_2$, then the graph has a zero eigenvalue if another node $n_3 \neq n_2 \neq n_1$ is connected to $S_1 \cup S_2$. These zero eigenvalues occur when a graph possesses a "local bi-partiteness". In real networks, this type of interconnection often occurs.

Lemma 10: For any effective spreading rate $\tau = \frac{\beta}{\delta} \geq 0$, the components $v_{i\infty}$ of the steady-state infection probability vector obey

$$\sum_{i=1}^{N} \left(d_i - \frac{1}{\tau} \right) v_{i\infty} = \sum_{j=1}^{N} \lambda_j(A) z_{j\infty}^2 \tag{28}$$

from which

$$0 \leq \sum_{j=1}^{N} \lambda_j(A) z_{j\infty}^2 \leq \sum_{i=1}^{N} \frac{|\tau d_i - 1|}{\tau d_i + 1} d_i \leq 2L$$

where L is the number of links.

Proof: The equality (28) is an immediate consequence of (27). The first upper bound follows from (15). The second one from the basic equation of the degree $\sum_{i=1}^{N} d_i = 2L$. □

Since $\sum_{j=1}^{N} \lambda_j(A) = 0$ for any graph, the lower bound in Lemma 10 shows that the positive eigenvalues and their eigenvectors are more important than the negative ones. Because the left hand side of (28) is increasing in τ, the vector V_∞ is increasingly more aligned with eigenvectors of A belonging to positive eigenvalues. Lemma 6 shows that at $\tau = \tau_c + \varepsilon$, only the eigenvector of $\lambda_{\max}(A)$ plays a role. As τ increases, we now deduce that V_∞ is influenced by additional eigenvectors (proportional to $\lambda_j(A)$). The contribution of the eigenvector of $\lambda_{\max}(A)$ to $\sum_{j=1}^{N} \lambda_j(A) z_{j\infty}^2$ remains dominant, because it is the only eigenvector with all positive components and all eigenvectors in U are normalized, i.e. $x_j^T x_j = 1$. By combining (28) and (18), we have

$$\sum_{j=1}^{N} \lambda_j(A) z_{j\infty}^2 = \frac{1}{\tau} \sum_{i=1}^{N} \frac{v_{i\infty}^2}{1 - v_{i\infty}}$$

VII. Evaluation of the Kephart and White model

In this section, we will show that, by making additional approximations, our model can reproduce the differential equation (1) of the Kephart and White model.

In a regular graph with degree k and adjacency matrix A_R, the degree vector $D = ku$ and the eigenvector belonging to the largest eigenvalue $\lambda_{\max}(A_R) = k$ is u such that (27) becomes

$$\frac{d}{dt}\left(u^T V(t)\right) = (\beta k - \delta) u^T V - \beta k \left(u^T V\right)^2 - \beta \sum_{j=2}^{N} \lambda_j(A_R) z_j^2$$

If we let $y(t) = \frac{u^T V}{N}$ and assume in the last sum that all eigenvalues and vectors are equal to the largest one, we again find the Kephart and White differential equation (1). Clearly, apart from the mean field approximation and the confinement to regular graphs (or nearly regular graphs), the Kephart and White model approximates the eigenvalue structure of a regular graph and only the largest eigenvalue and eigenvector are considered. Since $\sum_{j=1}^{N} \lambda_j(A_R) = 0$ implying that a non-negligible fraction of the eigenvalues are negative, the Kephart and White derivative $\frac{dy(t)}{dt}$ underestimates the actual rate of infection in the regular graph. Most likely, this underestimation is a general property of "homogeneous" virus spread models. A similar comment holds for the extended local models proposed by Pastor Satorras and Vespignani [13, Chapter 9].

For the simplest regular graph, the complete graph K_N, we observe that the equation (8) for each node i is identical. Thus, one might be led to put, $v_i = v_k$, for all $1 \leq k \leq N$ and for all t and such that $\sum_{j=1}^{N} a_{ij} v_j(t) = (N-1) v_i(t)$. In that case, the set of equations (9) reduces to a single equation,

$$\frac{dv_i(t)}{dt} = \beta(N-1) v_i(t) (1 - v_i(t)) - \delta v_i(t)$$

which is the Kephart and White differential equation (1). Although apparently correct, the assumption that $v_j = v_k$ (for all t) implies that all initial conditions also are the same. That full symmetry reduces the modeling of the network to that of a single node. Also, that local view of the single node is equivalent to ignoring all, but the largest eigenvalue in (27). In random attack strategies of computer viruses, where each node has equal probability to be infected initially, the full symmetry $v_i(0) = v_j(0)$ for any pair of nodes i and j is achieved.

VIII. Comparison of the N-intertwined MC with the exact 2^N -state MC

Via simulations, we assess the accuracy of the N-intertwined Markov chain. Only small networks are simulated because we expect for small N the largest error. Fig. 10,11 and 12 present a typically view of the fraction $y(t)$ as function of time t in K_{11} for three different τ-regimes.

Below the epidemic threshold $\tau_c = \frac{1}{10}$ ($N = 11$ in Fig. 10), the N-intertwined non-linear model is almost exact.

In a τ-region round τ_c, Fig. 11 illustrates that the deviations from the exact solution are substantial. But, sufficiently above τ_c as in Fig. 12, the accuracy of the N-intertwined non-linear model again improves. Since the N-intertwined non-linear model upperbounds the fraction of infected nodes as shown in Section IV-A, the relative small difference in Fig. 12 quantifies the effect of neglecting dependence in the mean field approximation.

In summary, for all graphs, if $\tau < \tau_c$, the N-intertwined Markov chain is very accurate. If $\tau > \tau_c$, the N-intertwined Markov chain differs from the exact solution, but the difference decreases with increasing network size N. The fact that

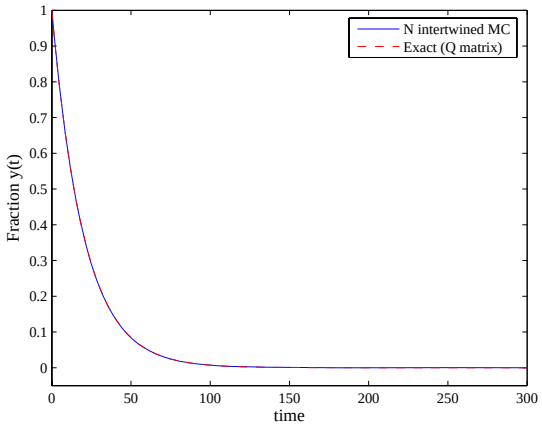

Fig. 10. The fraction $y(t)$ of infected nodes in K_{11} where $\tau = 10^{-3}$ as a function time computed exactly (via the Q-matrix) and with the N intertwined Markov chain model.

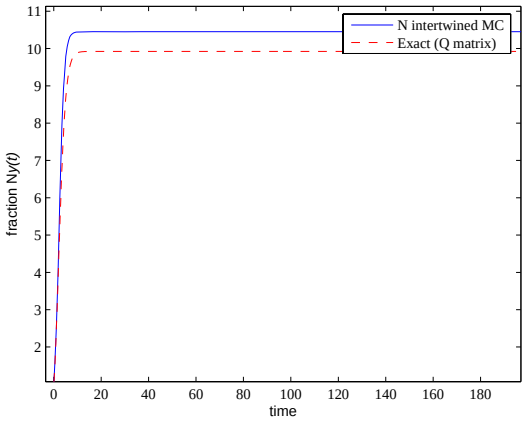

Fig. 12. The N times the fraction $y(t)$ of infected nodes in K_{11} where $\tau = 2$ as a function time computed exactly (via the Q-matrix) and with the N intertwined Markov chain model.

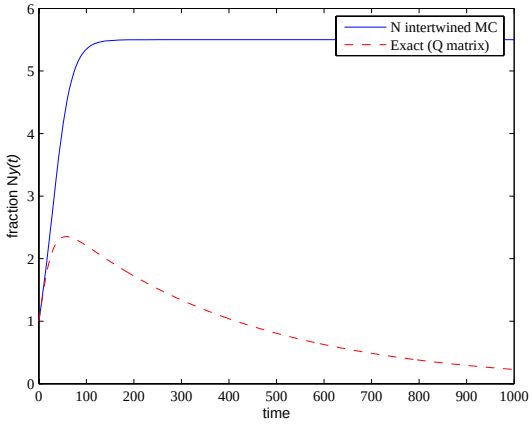

Fig. 11. The $N = 11$ times the fraction $y(t)$ of infected nodes in K_{11} where $\tau = 0.2 = 2\tau_c$ as a function time computed exactly (via the Q-matrix) and with the N intertwined Markov chain model.

the non-linear N-intertwined model and the exact 2^N-state Markov chain are close for large N is linked with a general property of Markov chains: A Markov chain can approximate any stochastic process arbitrarily close provided the number of states in the Markov chains is sufficiently large.

IX. Conclusions

The robustness of the infrastructure against failures and attacks has motivated the analysis of an epidemic spreading process in a given, fixed network, represented by the adjacency matrix A. Individual interactions are not homogeneous, but dictated by the structure of the network. Models of spreading processes should take the network topology into account.

Two models for virus spread in networks are presented: the exact 2^N state Markov chain and the new N-intertwined model, whose only approximation lies in the application of mean field theory. The exact Markov chain provides insight into the virus spread process (the time of convergence to the absorbing state). The N-intertwined model relates network topology parameters to the spreading process (largest eigenvalue and degrees of the nodes). The influence of the mean field approximation is quantified. Several upper bounds for the steady-state infection probabilities are presented.

Additional contributions of the paper are: (a) Our N-intertwined model reduces for regular graphs to the basic Kephart and White epidemiological model after additional simplifications. (b) We have explored the phase transition phenomenon and shown that, for a fixed graph, the epidemic threshold τ_c is consequence of the mean field approximation. We have presented the relation between spreading rate τ and convergence time towards the extinction of epidemics for two extreme cases (full mesh and line graph). This is especially important for smaller epidemics where τ is close to the epidemic threshold and where the lifetime of an epidemic varies significantly. (c) The largest eigenvalue of the adjacency matrix of the graph is rigorously shown to define an epidemic threshold of the N-intertwined model (as well as of other mean field models).

Acknowledgement

This research was supported by the Netherlands Organization for Scientific Research (NWO) under project number 643.000.503 and by Next Generation Infrastructures (Bsik).

References

[1] Albert, R. and H. Jeong and A.-L. Barabsi, "Error and Attack Tolerance of complex networks", Nature Vol. 406, pp. 378-382, 27 July, 2000.

[2] C. Asavathiratham, "The Influence Model: A Tractable Representation for the Dynamics of Networked Markov Chains", Phd thesis Massachusetts Institute of Technology, October 2000.

[3] N. T. J. Bailey, *The Mathematical Theory of Infectious Diseases and its Applications*, Charlin Griffin & Company, London, 2nd ed., 1975.

[4] G. S. Canright and K. Engo-Monsen, "Spreading on Networks: A Topographic View", Complexus2006.

[5] D. M. Cvetkovic, M. Doob, and H. Sachs, "Spectra of graphs, Theory and Applications", Johan Ambrosius Barth Verlag, Heidelberg, third edition, 1995.

[6] D. J. Daley and J. Gani, *Epidemic modelling: An Introduction*, Cambridge University Press, 1999.

[7] G. F. D Duff and D. Naylor, *Differentiation equations of applied mathematics*, John Wiley & Sons, 1966.

[8] R. Durrett and X.-F. Liu, "The contact process on a finite set", The Annals of Probability, Vol. 16, No. 3, pp. 1158-1173, 1988.
[9] A. Ganesh, L. Massoulié and D. Towsley, "The Effect of Network Topology on the Spread of Epidemics", IEEE INFOCOM2005.
[10] M. Garetto, W. Gong, D. Towsley, "Modeling Malware Spreading Dynamics", IEEE INFOCOM'03, San Francisco, CA, April 2003.
[11] J. O. Kephart and S. R. White, "Direct-graph epidemiological models of computer viruses", Proceedings of the 1991 IEEE Computer Society Symposium on Research in Security and Privacy, pp. 343-359, May 1991.
[12] R. Pastor-Satorras and A. Vespignani, "Epidemic Spreading in Scale-Free Networks", Physical Review Letters, Vol. 86, No. 14, April, 3200-3203.
[13] R. Pastor-Satorras and A. Vespignani, *Evolution and Structure of the Internet, A Statistical Physics Approach*, Cambridge University Press, 2004.
[14] P. Van Mieghem, *Performance Analysis of Communication Systems and Networks*, Cambridge University Press, 2006.
[15] Y. Wang, D. Chakrabarti, C. Wang, and C. Faloutsos, "Epidemic Spreading in Real Networks: An Eigenvalue Viewpoint", In 22nd International Symposium on Reliable Distributed Systems (SRDS'03), pp. 25–34. IEEE Computer, October 2003.
[16] Y. Wang and C. Wang, "Modeling the Effects of Timing Parameters on Virus Propagation", ACM Workshop on Rapid Malcode (WORM'03), Washington DC, Oct. 27, p. 61-66, 2003.

APPENDIX

We compute the upper bound of the sum of the rows in Q for the line topology. First, let us consider two cases with the same number of infected nodes on the same line graph as shown in Fig. 13.

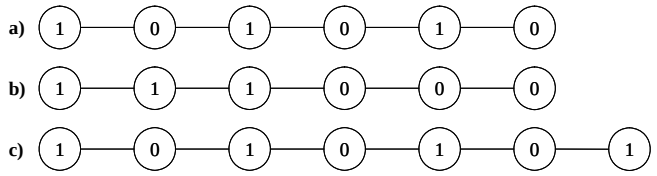

Fig. 13. a) and b): Line graph with $N = 6$ and 3 infected nodes. The '1 ' refers to an infectected and a '0 ' to healthy node. c) Line graph with $N = 7$ (odd number of nodes) and 4 infected nodes.

Case a) has two nodes that can be infected by two neighbors and one that can be infected by only one neighbor. In the case b) only one node can be infected by one neighbor. Thus, in the case a) all healthy nodes can be infected by two neighbors in contrast to case b) where one node can be infected by only one neighbor. Since, from the viewpoint of curing, both cases are equal, we will consider only the cases analogous to a), where nodes are alternately infected. There is also a difference between the line graphs with odd and even number of nodes N, as observed from case c). We can now write the sum of the non-diagonal elements of such a i-th row in Q as a function of the number of infected nodes k. We have for odd N,

$$\max|q_{ii}| = (2\beta(k-1) + \beta + \delta k), \qquad k < \frac{N+1}{2}$$

$$\max|q_{ii}| = (2\beta(N-k) + \delta k), \qquad k \geqslant \frac{N+1}{2}$$

and when N is even,

$$\max|q_{ii}| = (2\beta(k-1) + \beta + \delta k), \qquad k \leqslant \frac{N}{2}$$

$$\max|q_{ii}| = (2\beta(N-k) + \delta k), \qquad k > \frac{N}{2}$$

PLACE PHOTO HERE

P iet Van Mieghem is professor at the Delft University of Technology with a chair in telecommunication networks and chairman of the section Network Architectures and Services (NAS). His main research interests lie in new Internet-like architectures for future, broadband and QoS-aware networks and in the modelling and performance analysis of network behavior and complex infrastructures. Professor Van Mieghem received a Master's and Ph. D. in Electrical Engineering from the K.U.Leuven (Belgium) in 1987 and 1991, respectively. Before joining Delft, he worked at the Interuniversity Micro Electronic Center (IMEC) from 1987 to 1991. During 1993 to 1998, he was a member of the Alcatel Corporate Research Center in Antwerp where he was engaged in performance analysis of ATM systems and in network architectural concepts of both ATM networks (PNNI) and the Internet.
He was a visiting scientist at MIT (department of Electrical Engineering, 1992-1993) and, in 2005, he was visiting professor at ULCA (department of Electrical Engineering). He was member of the editorial board of the journal Computer Networks from 2005-2006.

PLACE PHOTO HERE

J asmina Omic is a PhD student in Delft University of Technology, the NAS group (faculty of Electrical Engineering, Mathematics and Computer Science), under the supervision of Professor Van Mieghem. Her focus is on modeling of virus spread, denial of service attacks and other malicious actions exerted on a communication infrastructure. She graduated from the Faculty of Electrical Engineering, University of Belgrade, with major in electronics, telecommunications and control in 2005. After her graduation, she has been working with several telecommunication companies in Belgrade on Internet security.

PLACE PHOTO HERE

R obert Kooij obtained his PhD in 1993 from the Delft University of Technology (the Netherlands). His thesis dealt with qualitative theory of differential equations.

After defending his PhD thesis he spent four years as a free lance mathematician. Since August 1997 he is working as an innovator at TNO ICT (the former KPN Research). His main research interest is Quality of Service aspects (such as delay, packet loss and throughput) of telecommunication networks which are based on IP technology. Apart from QoS at the network level he is also working on quality as experienced by users, both for voice, video and data services. Currently he is active both in national research projects and in European projects such as MUSE (Multi Service Access Everywhere, part of the 6th Framework Programme). He is also working on consultancy projects for telecom operators. His research has lead to several publications, mainly on modelling Voice over IP, video quality and TCP throughput. He also regularly gives guestlectures on telecommunications at universities throughout the Netherlands.

Since November 2005 he is a part-time associate professor in the Network Architectures and Services group where he works on the NWO project ROBUNET which deals with the robustness of large scale networks. Dr. Kooij has published about 50 papers in journals and conference proceedings.